ELSEVIER

Physica E 6 (2000) 214–217

PHYSICA E

www.elsevier.nl/locate/physe

X_X–X_Y interface band mixing in GaAs/AlAs heterostructures

Hyunsik Im[a], L.E. Bremme[a], Y.C. Chung[a], P.C. Klipstein[a,*], R. Grey[b], G. Hill[b]

[a] *Clarendon Laboratory, Department of Physics, University of Oxford, Parks Road, Oxford, OX1 3PU, UK*
[b] *Department of Electrical & Electronic Engineering, University of Sheffield, Mappin Street, Sheffield SI 3JD, UK*

Abstract

The in-plane dispersion of the $X_{X,Y}$ states in a GaAs/AlAs "double-barrier structure" is measured by varying the angle of an in-plane magnetic field. When $X_{X,Y}$ (1) states in the emitter AlAs layer tunnel into collector $X_{X,Y}$ ($m > 1$) states, a characteristic dumbbell shape is observed for the bias shift of the resonant tunneling peak versus magnetic field angle, with the major axis along [1 1 0] or [$\bar{1}$ 1 0]. This corresponds to an elliptical constant energy surface in the collector AlAs layer which is rotated by 45° with respect to the bulk Fermi surface. We explain the new symmetry by X_X–X_Y interface band mixing which is closely analogous to the widely studied Γ–X_Z mixing. Our results provide new insight into the microscopic origin of both types of mixing.

PACS: 73.20.Dx; 73.40.Gk; 71.18.+y

Keywords: Double barrier structure; Interface band mixing

1. Introduction

About 10 years ago it was predicted that in GaAs/AlAs heterostructures grown along [0 0 1] (z-direction), it is possible for mixing to occur between the AlAs X_X and X_Y conduction band edge states, located near the four in plane $\langle 1\,0\,0 \rangle$ boundaries of the bulk Brillouin zone [1]. In this paper we show that the effect of the mixing on the in-plane dispersion can be dramatic, particularly when an electric field is applied in the z-direction to break the four-fold symmetry in the plane. At the band edge, the four ellipses oriented along [1 0 0] and [0 1 0], which form the X_X and X_Y constant energy surfaces, are then replaced by a single elliptical surface oriented along either [1 1 0] or [$\bar{1}$ 10]. Using resonant magneto-tunneling, we are able to measure the in-plane dispersion which, to the best of our knowledge, constitutes the first observation of X_X–X_Y mixing. We estimate the values of the mixing potentials associated with Bloch states of X_1 and X_3 symmetry, respectively. We show that *interference* between these two contributions to the overall mixing potential is directly responsible for the new symmetry of the constant energy surface. Contrary to a recent

* Corresponding author. Fax: 44-1865-272400.
E-mail address: p.klipstein@physics.ox.ac.uk (P.C. Klipstein)

1386-9477/00/$ - see front matter
PII: S1386-9477(99)00082-X

theory, our results show that the X_1 related potential is finite.

2. Experimental

We have studied 2D $\rightarrow$ 2D tunnelling between confined states in a GaAs/AlAs structure comprising two 70 Å wide AlAs wells separated by a 30 Å wide GaAs barrier, surrounded by 150 Å spacers and doped GaAs contacts. The $Ga_{1-x}Al_xAs$ region before each spacer has been graded linearly over a distance of 1000 Å from $x = 0$–0.1 to enable efficient electron transfer from Γ states in the graded region to ground $X_{X,Y}$ states in the emitter well. Fig. 1 shows the band profile in a typical structure (without grading) when the $X_{X,Y}$ (1) emitter state is in resonance with the $X_{X,Y}(3)$ collector state. The conductance is plotted versus bias in Fig. 2. $X_{X,Y}(1) \rightarrow X_{X,Y}(m)$ processes responsible for the peaks, where m is the confinement quantum number, are identified in Fig. 2 by comparison with a similar ungraded sample, in which the emitter $X_{X,Y}$ states were populated using a pressure of ~9 kbar [2].

The dispersions of the $X_{X,Y}$ states were studied by applying an in-plane magnetic field which introduces a change in wave vector during tunneling, $\Delta k_y = -eB_x\Delta z/\hbar$, where Δz is the distance between emitter and collector wave functions [3–6]. For the present sample at 15 T, $\Delta k_y \sim 0.02 \times 2\pi/a_0$, where a_0 is the cubic lattice constant. The resulting shift in bias allows the dispersion in the collector to be mapped out. Fig. 2 shows the shift for the $X_{X,Y}(1) \rightarrow X_{X,Y}(3)$ peak as the field is increased in the [1 0 0] direction. When the shift is plotted versus the angle of the in-plane field, a characteristic dumbbell shape is observed, as shown in Fig. 3, corresponding to an elliptical constant energy surface with its principal axes along [1 1 0] and [$\bar{1}$ 1 0]. We have also observed similar behaviour in a 60–40–60 Å sample [7]. For the sample of Fig. 3, the dumbbell axis is identical for both bias directions, although in reverse bias the ratio of the

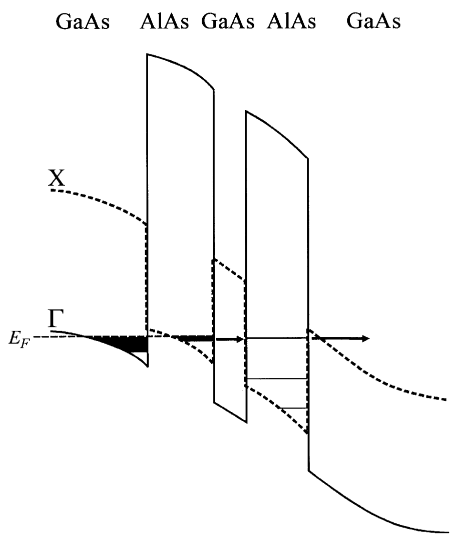

Fig. 1. Band profile at the $X_{X,Y}(1) \rightarrow X_{X,Y}(3)$ resonance.

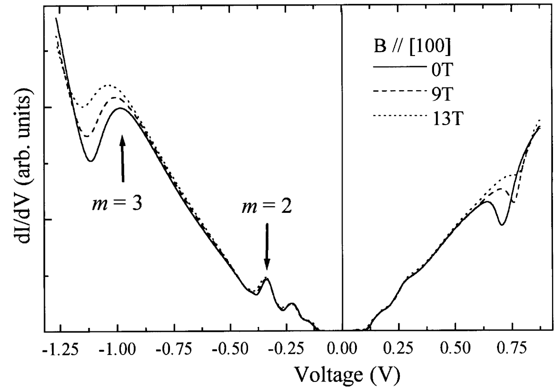

Fig. 2. Conductance versus bias at 4.2 K. A magnetic field is applied in the [1 0 0] direction.

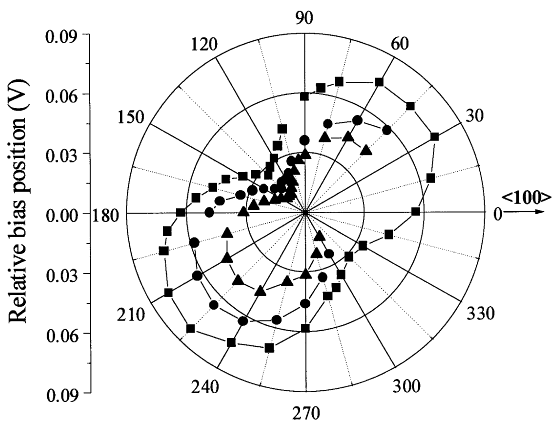

Fig. 3. Bias shift of the reverse bias $X_{X,Y}(1) \rightarrow X_{X,Y}(3)$ peak in Fig. 1 with angle of the in-plane magnetic field. Triangles, circles and squares are for 12, 13.5 and 15 T, respectively.

shifts for the two $\langle 1\,1\,0\rangle$ magnetic field directions is significantly larger (~ 2.8 at 15 T) than in forward bias (~ 1.6 at 10.5 T). This ratio varied between different mesas from the same wafer, particularly in reverse bias, where for three mesas the largest value at 15 T was 2.8, and the smallest 1.9.

3. Discussion

The bulk X_X and X_Y states have Camel's back dispersions in the (k_x, k_y) plane:

$$E_X = \frac{\hbar^2}{2}\left[\frac{k_x^2}{m'_Z} + \frac{k_y^2}{m_{X,Y}}\right] - E_{\boldsymbol{k}.\boldsymbol{p}}(k_x)$$

and

$$E_Y = \frac{\hbar^2}{2}\left[\frac{k_x^2}{m_{X,Y}} + \frac{k_y^2}{m'_Z}\right] - E_{\boldsymbol{k}.\boldsymbol{p}}(k_y),$$

where $E_{\boldsymbol{k}.\boldsymbol{p}}(k_\sigma) = \sqrt{(\Delta/2)^2 + R^2k_\sigma^2}$. Δ is the splitting at the X-points between the bands with X_1 and X_3 symmetry, and R, m'_Z are $\boldsymbol{k}.\boldsymbol{p}$ parameters [8]. In the heterostructure it has been shown that the interfaces can mix the X_X and X_Y states with a potential: $V(k_x,k_y) = b^*(k_x)b(k_y)\bar{V}_1^{\mathrm{X-Y}} + a^*(k_x)a(k_y)\bar{V}_3^{\mathrm{X-Y}}$ where $b(k_\sigma) = \sqrt{0.5 + \Delta/4E_{\boldsymbol{k}.\boldsymbol{p}}}$ and $a(k_\sigma) = i\,\mathrm{sgn}(k_\sigma)\sqrt{0.5 - \Delta/4E_{\boldsymbol{k}.\boldsymbol{p}}}$ [7–9]. Here, $\bar{V}_1^{\mathrm{X-Y}} = \beta_1\Sigma_{z_i}\Xi_X^*(z_i)\Xi_Y(z_i)\exp(\mathrm{i}2\pi z_i/a_0)$ and $\bar{V}_3^{\mathrm{X-Y}} = \beta_3\Sigma_{z_i}\Xi_X^*(z_i)\Xi_Y(z_i)P(z_i)\exp(\mathrm{i}2\pi z_i/a_0)$ are mixing potentials in which $\Xi_{X,Y}(z)$ are envelope functions of the unmixed $X_{X,Y}$ states, $\beta_1 < \beta_3$ are constants related to the interface potential, a_0 is the cubic lattice parameter, z_i are the interface positions and $P(z_i) = 1(-1)$ for AlAs on GaAs (GaAs on AlAs) [7–10]. The energies of the mixed states are obtained by diagonalising the Hamiltonian:

$$H_{XY} = \begin{bmatrix} E_X & V \\ V & E_Y \end{bmatrix}.$$

In Fig. 4, we plot the dispersion and constant energy contours in the (k_x, k_y) plane using the $\boldsymbol{k}.\boldsymbol{p}$ parameters $R = 1$ eV Å, $\Delta = 0.35$ eV, $m'_Z/m_e \approx 1.56$ of Ref. [8], and potentials $\bar{V}_1^{\mathrm{X-Y}} = 30$ meV, $\bar{V}_2^{\mathrm{X-Y}} = 850$ meV. We take $m_{X,Y}/m_e = 0.24$ [2,11]. It can be seen that the contours are elliptical with their major axis along [1 1 0]. The sub-band kinetic energy in Fig. 4 at constant $k_{||}$ should be proportional to the bias shift plotted in Fig. 3 when $\boldsymbol{k}_{||}$ is at right angles to the magnetic field. In Fig. 5, we show kinetic energy plots for $\boldsymbol{k}_{||} = 0.02 \times 2\pi/a_0$ with $\bar{V}_1^{\mathrm{X-Y}} = 6$ or 30 meV and $\bar{V}_3^{\mathrm{X-Y}} = 850$ meV. The value of $\bar{V}_3^{\mathrm{X-Y}}$ was chosen by noting that the ratio of kinetic energies for the two $\langle 1\,1\,0\rangle$ directions is very sensitive to $\bar{V}_3^{\mathrm{X-Y}}$. Fig. 5 shows that $\bar{V}_1^{\mathrm{X-Y}}$ hardly affects this ratio but it does influence the shape of the kinetic energy plot. We find good correspondence between Figs. 3 and 5(b) suggesting that for these $\boldsymbol{k}.\boldsymbol{p}$ parameters, $\bar{V}_1^{\mathrm{X-Y}}$ ~30 meV is a good estimate for the collector well of the 70–30–70 sample in reverse bias.

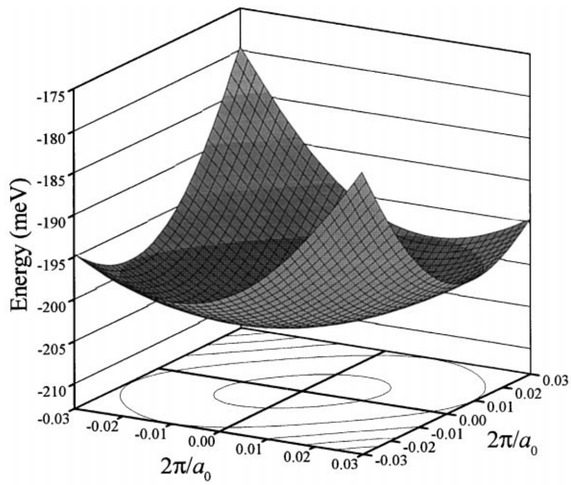

Fig. 4. Dispersion and energy contours in the (k_x, k_y) plane of an X_1 quantum well, calculated using $\bar{V}_1^{\mathrm{X-Y}} = 30$ meV, $\bar{V}_3^{\mathrm{X-Y}} = 850$ meV. The zero of energy is midway between the bulk X_1 and X_3 edges.

The $\langle 1\,1\,0\rangle$ orientation of the elliptical contours in Fig. 3 is due to interference between the $\bar{V}_1^{\mathrm{X-Y}}$ and $\bar{V}_3^{\mathrm{X-Y}}$ terms in the expression for $V(k_x, k_y)$, since $a^*(k_x)a(k_y) > 0$ for $\boldsymbol{k}_{||}$ along [1 1 0] but $a^*(k_x)a(k_y) < 0$ for $\boldsymbol{k}_{||}$ along [$\bar{1}$ 1 0]. The interference shows that both mixing potentials are finite. A finite $\bar{V}_1^{\mathrm{X-Y}}$ is consistent with Ref. [1] but not with Ref. [10] which predicts $\beta_1 = 0$. The result $\bar{V}_1^{\mathrm{X-Y}} < \bar{V}_3^{\mathrm{X-Y}}$ is consistent with theory [9,10,12], while the relatively large size of both $\bar{V}_1^{\mathrm{X-Y}}$ and $\bar{V}_3^{\mathrm{X-Y}}$ is due in part to the large amplitudes of Ξ_X and Ξ_Y at the last interface of the collector quantum well. Even so, we

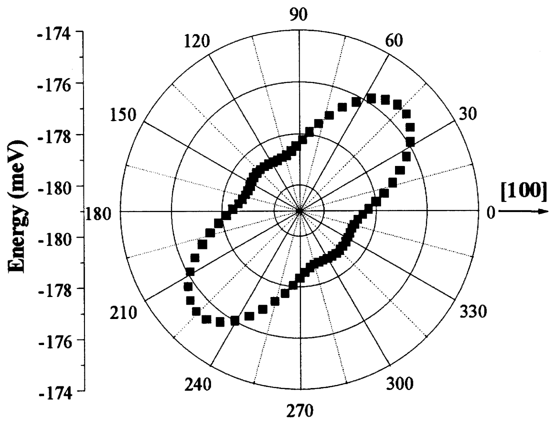

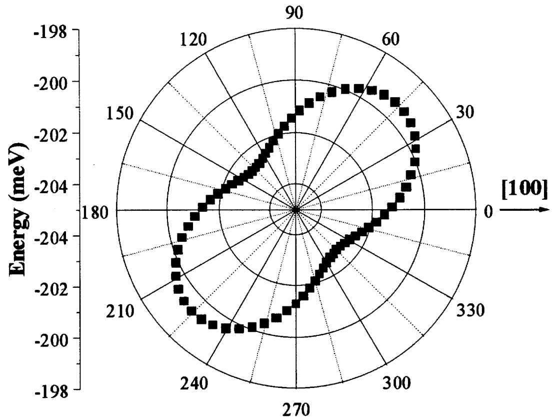

Fig. 5. Kinetic energy at $\boldsymbol{k}_{||} = 0.02 \times 2\pi/a_0$ for field angles in the (k_x, k_y) plane, calculated with $\bar{V}_3^{\mathrm{X-Y}} = 850\,\mathrm{meV}$ and (a) $\bar{V}_1^{\mathrm{X-Y}} = 6\,\mathrm{meV}$ (b) $\bar{V}_1^{\mathrm{X-Y}} = 30\,\mathrm{meV}$. Zero angle corresponds to [1 0 0].

note that β_3 is much greater than the expected range of $\sim 0.5\,\mathrm{eV\,Å}$ estimated in Ref. [10]. Therefore, we have re-examined the $\boldsymbol{k.p}$ parameters and find that $R \sim 2.5\,\mathrm{eV}$ Å and $m_Z'/m_{\mathrm{e}} \sim 0.3$ are consistent with recently measured confinement energies for X_Z states in narrow quantum wells [7,13], whereas those in Ref. [8] are not. With these new parameters we obtain a fit to the angular dependence of the kinetic energy virtually identical to that in Fig. 5(b), but with $\bar{V}_1^{\mathrm{X-Y}} = 30\,\mathrm{meV}$, $\bar{V}_3^{\mathrm{X-Y}} = 120\,\mathrm{meV}$. These potentials yield a β_1 value comparable with $\sim 0.4\,\mathrm{eV}$ Å deduced from tight binding calculations in Ref. [1], but β_3 is still several times greater than expected [7,10]. It suggests that further refinement might be needed for the envelope function theory of interface band mixing.

In conclusion we have observed the first clear evidence for mixing between AlAs X_X and X_Y states predicted in Ref. [1]. We have shown that the mixing leads to a rotation of the constant energy surface from the two in-plane $\langle 1\,0\,0\rangle$ directions to one of the $\langle 1\,1\,0\rangle$ directions. Which of the $\langle 1\,1\,0\rangle$ directions depends on the details of the interface structure and the bias conditions. The rotation is a consequence of interference between the X_1 and X_3 contributions to the mixing potential. This shows that β_1 cannot be zero, as recently suggested in Ref. [10]. We find $\bar{V}_3^{\mathrm{X-Y}} > \bar{V}_1^{\mathrm{X-Y}} \sim 30\,\mathrm{meV}$ in the collector well of our *biased* sample. By considering the microscopic interface potential, a close analogy exists between X_X–X_Y and Γ–X_Z mixing [9]. It follows that the X_1 related Γ–X_Z mixing potential must also be finite, contrary to the models in Refs. [8,12].

References

[1] Y.-T. Lu, L.J. Sham, Phys. Rev. B 40 (1989) 5567.
[2] J.M. Smith et al., Phys. Rev. B 57 (1998) 1740.
[3] B.R. Snell et al., Phys. Rev. Lett. 59 (24) (1987) 2806.
[4] J. Smoliner et al., Phys. Rev. Lett. 63 (1989) 2116.
[5] R.K. Hayden et al., Phys. Rev. Lett. 66 (1991) 1749.
[6] J.M. Smith et al., Phys. Rev. B 58 (1998) 4708.
[7] H. Im, P.C. Klipstein, R. Grey, G. Hill, Phys. Rev. Lett. 83 (1999) 3693.
[8] Y. Fu et al., Phys. Rev. B 47 (1993) 13 498.
[9] P.C. Klipstein, in: M. Heiblum, E. Cohen (Eds.), 24th International Conference on Physics of Semiconductors, Jerusalem, 1998, World Scientific, Singapore, 1999, CDROM 1265.pdf.
[10] B.A. Foreman, Phys. Rev. Lett. 81 (1998) 425.
[11] H. Im, P.C. Klipstein, R. Grey, G. Hill, in: M. Heiblum, E. Cohen (Eds.), 24th International Conference on Physics of Semiconductors, Jerusalem, 1998, World Scientific, Singapore, 1999, CDROM 1075.pdf.
[12] T. Ando, H. Akera, Phys. Rev. B 40 (1989) 11 619.
[13] H. Im, P.C. Klipstein, J.M. Smith, R. Grey, G. Hill, Phys. Stat. Sol. 211 (1998) 489.